

## CALORIMETRIC DETERMINATION OF THE ENTHALPIES OF FORMATION OF LIQUID Ni–Ti ALLOYS

R LUCK and I ARPSHOFEN

*Max-Planck-Institut für Metallforschung, Institut für Werkstoffwissenschaften,  
Seestr 75, D-7000 Stuttgart 1 (F R G)*

B PREDEL

*Max-Planck-Institut für Metallforschung, Institute für Werkstoffwissenschaften,  
and  
Institut für Metallkunde der Universität Stuttgart, Seestr 75, D-7000 Stuttgart 1 (F R G)*

J F SMITH

*Ames Laboratory, U S Dept of Energy, and Department of Metallurgy and Materials Science,  
Iowa State University, Ames, IA 50011 (U S A)*

(Received 1 December 1987)

### ABSTRACT

The enthalpies of formation of liquid Ni–Ti alloys have been measured independently with two different calorimeters, one set at 1741 and the other at 1838 K. Measurements were made within the composition range  $0 < X_{\text{Ti}} < 0.5$  where  $X_{\text{Ti}}$  is the mole fraction of Ti. A minimum in the compositional dependence of  $\Delta_{\text{M}}H$  between  $X_{\text{Ti}} = 0.3$  and  $X_{\text{Ti}} = 0.4$  shows definitively that the solution is not regular. Rather there is indication that atomic packing considerations lead to the persistence of short-range order in the liquid phase above and in the vicinity of the efficiently packed intermetallic phase at  $\text{Ni}_3\text{Ti}$ .

### INTRODUCTION

The Ni–Ti system is of both technologic and scientific interest. Poole and Hume-Rothery [1] investigated the phase relationships in the system and combined their results with earlier data to propose the phase diagram which is currently accepted. This diagram is shown in Fig. 1 and shows three intermediate phases:  $\text{Ni}_3\text{Ti}$  which melts congruently near  $1380^\circ\text{C}$  and whose structure is a hexagonal closed-packed superlattice [2,3],  $\text{NiTi}$  which melts congruently near  $1310^\circ\text{C}$  and which has the CsCl-type structure [4,5] at elevated temperatures, and  $\text{NiTi}_2$  which melts peritectically near  $984^\circ\text{C}$  and which has a complex cubic structure [5–8] with 96 atoms per unit cell.

Extensive research on the system has been stimulated by the unusual martensitic transformation [9–11] that has been found in alloys near

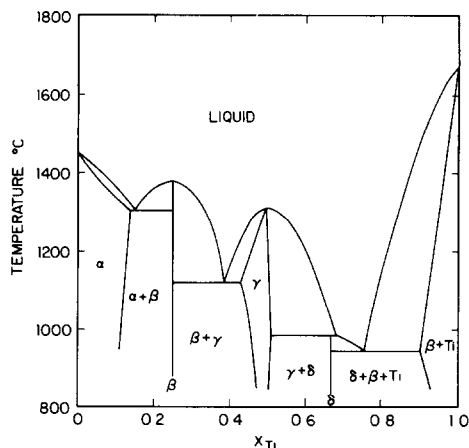


Fig 1 The Ni-Ti phase diagram (after Poole and Hume-Rothery)

equiatomic stoichiometry. This transformation is associated with the 'shape memory' effect that has led to a variety of practical applications for these alloys, the most extensive of which have been for the coupling of tubing and piping [12]. Additional stimulation for the research has come from the finding that alloys on the Ti-rich side of the diagram, particularly through the composition range 60–70 atm% Ti, have glass-forming ability [13–15], and near the stoichiometry  $\text{NiTi}_2$  a metastable quasicrystal phase can be formed [16]. However, in spite of the extensive amount of research carried out so far on this system, thermodynamic research has been limited to seven investigations.

As might be expected, the majority of these thermodynamic investigations [11,17–19] (four out of seven) have been concerned with the thermodynamics of the martensitic transformation in the NiTi phase, one [15] has been concerned with the glass phase. Values from  $1300 \text{ J (mol atoms)}^{-1}$  ( $1/2 \text{ mol NiTi}$ ) to  $2100 \text{ J (mol atoms)}^{-1}$  for the heat of this martensitic transition from four independent measurements have been reported. The scatter seems attributable to the degree with which the reaction goes to completion and to composition variation associated with a finite width of the NiTi phase field. There is also disagreement [18,19] as to whether the transformation is first [18] or higher order [19], although the two investigations which disagree agree that the heat capacity of the phase at temperatures immediately above the transition is of the order of  $24\text{--}25 \text{ J K}^{-1} (\text{mol atoms})^{-1}$ .

Two investigations of the enthalpies of solid alloy formation have been made. The first of these by Kubaschewski [20] measured the heats of formation of nineteen alloys across the complete composition range of the Ni-Ti system by heating unreacted powders of the components to a temperature above the onset of rapid reaction, the enthalpy of formation at ambient temperature was evaluated by comparing the energy cost during the

reaction run to the post-reaction energy cost of heating the reacted material from the same initial temperature to the same maximum temperature reached during the reaction run

The second investigation of the enthalpies of solid alloy formation was by Gachon and coworkers [21,22]. The measurements were of the enthalpies of alloy formation of the three intermediate phases in the system and were measurements of the direct reactions at temperature slightly below the melting points of the intermediate phases. This second investigation was carried out in an integrated heat flux calorimeter [23] with a SETARAM furnace, qualitatively quite similar to the calorimeters used in our investigation. Comparison of the results between the two investigations shows quite good agreement between the values for the enthalpies of formation for  $\text{NiTi}$  and  $\text{NiTi}_2$ , but a difference between the values for the enthalpy of formation of  $\text{Ni}_3\text{Ti}$  well outside the precision of measurement. Gachon and coworkers speculated that this difference might be attributable to a difference in the completeness of reaction in the two sets of measurements.

The present investigation was undertaken to measure the enthalpies of alloy formation as a function of composition in the liquid phase of the  $\text{Ni-Ti}$  system. At the elevated temperatures associated with liquid stability the completeness of any mixing reaction should not be a problem because kinetics of reaction in the liquid state are much faster than in the solid state.

## PROCEDURE AND RESULTS

Heats of mixing of the pure liquid metals were measured in two different calorimeters. Both calorimeters were of the integrated heat flux type. The first calorimeter (the SETARAM calorimeter) operated under a slight positive pressure of pure argon and utilized a graphite heating element for maintaining its reference heat reservoir at constant temperature. The second calorimeter (the vacuum calorimeter) operated with a vacuum environment of the order of  $\sim 3 \times 10^{-5}$  mbar and utilized a molybdenum heating element for the maintenance of a constant temperature in its heat reservoir. A detailed description of the SETARAM calorimeter is available from SETARAM of Lyon, France, and its application has been described [24,25]. A description of the construction and operation of the vacuum calorimeter has also been published [26].

The calibration procedure for the SETARAM calorimeter is described in some detail because of significant differences from the procedure of previous publications [24,25]. The sensitivity of the calorimeter is not constant but, because of geometrical considerations, varies from crucible to crucible and depends upon the height to which the crucible is filled. The height, of course, increases with successive additions of sample material during a series of measurements. The sensitivity is a function of the distance from the

center of the thermic event in the crucible to the upper circle of thermocouples of the thermophile sensor. The shoulder of the outer wall of the crucible rests on these thermocouples. The sensitivity thus increases from rather low values at zero bath height to a maximum when the bath level reaches the level of the upper thermophile circle. The reverse of the sensitivity, the calibration factor, can be described as a function of the bath height by a parabola of second degree.

Calibration is usually effected by adding inert samples into the calorimeter. Since there was a question as to whether the previously used calibration substances ( $W$ ,  $Al_2O_3$ ) were sufficiently inert to a  $Ni-Ti$  bath, pure  $Ni$  itself was used in both calorimeters to calibrate heat transfer between crucible and heat reservoir. This was accomplished by dropping  $Ni$  samples into a liquid  $Ni$  bath. The initial bath consisted of  $\sim 1$  g  $Ni$  in the SETARAM calorimeter and  $\sim 25$  g  $Ni$  in the vacuum calorimeter. For the SETARAM calorimeter, comparison of earlier calibration data with inert materials with data from calibration with pure  $Ni$  showed that a parabolic form was also valid for the  $Ni$  calibration curve.

The heat of mixing for the alloys was measured by dropping  $Ti$  samples into an initially pure  $Ni$  bath with successive samples building the  $Ti$  concentration. Samples were dropped from room temperature and data for correcting for the heat necessary to raise the samples to bath temperature and for the fusion of the samples were taken from the compilation of Hultgren et al. [27]. Alumina crucibles were used in both calorimeters for containing the metal baths. At the temperatures of measurement in the calorimeters, standard Gibbs energy data [28] for the reduction reactions of  $Al_2O_3$  by either  $Ni$  or  $Ti$  are both positive but for the  $Ti$  reaction only weakly so. Further, at the temperatures in question, the vapor pressure [29] of  $Al$  is significant so that the tendency to escape of any  $Al$  that is formed will tend to drive the reduction reaction. Thus we anticipated that some reaction between melt and crucible might occur at higher  $Ti$  activities as the concentration of  $Ti$  in the melt increased with successive  $Ti$  additions.

Titanium was obtained from the Titanium Metal Corporation and nickel was obtained from the International Nickel Company. These materials were separately first arc melted and then electron beam melted. Samples for the SETARAM calorimeter were prepared in the form of small, nearly-cubic prisms with a mean edge length of about 0.28 cm, thus weighing, in the average, somewhat less than 0.2 g ( $Ni$ ) or about 0.1 g ( $Ti$ ). The shape was achieved by first rolling the metal and then dicing the rolled sheet with a diamond saw. Somewhat larger samples ( $\sim 1$  g) were prepared for the vacuum calorimeter by swaging a solidified melt and then slicing the swaged rods. All samples were stress relieved at  $\sim 950^\circ C$  for approximately 2 h under a vacuum of  $10^{-5}$ – $10^{-6}$  mbar. Analytical data for the content of interstitial elements in the unreacted  $Ni$  and  $Ti$  metals used in the measurements are shown in Table 1. These data are based on vacuum fusion

TABLE 1

Analyses for interstitial content in ppm by wt of sample materials before alloying and of alloys produced in the SETARAM and vacuum calorimeters during measurements of the enthalpies of alloy formation

Material	O	H	N	C
Ni samples	20	<sup>a</sup>	4	41
Ti samples	230	4	30	36
Ni-Ti alloy from first SETARAM run	14000	1300	20000	2400
Ni-Ti alloy from second SETARAM run	9000	800	29000	380
Ni-Ti alloy from vacuum calorimeter	2600	35	100	10

<sup>a</sup> Below detectable limit

analyses for oxygen, hydrogen, and nitrogen and combustion analyses for carbon. Values are in ppm by wt.

Measurements were made in the SETARAM calorimeter at 1741 K, and in the vacuum calorimeter at 1838 K. With current technology and construction materials, these temperatures are near the upper limit of conventional calorimetry. Two runs were made with the SETARAM calorimeter, but the first of these was erratic and was discarded. Post-run analyses from this first run showed appreciable reaction of the metal with the interstitial contaminants, namely O, H, N and C, and analytical results are included in Table 1. Further, post-run macro-examination showed pipes or voids and microstructural examination indicated appreciable inhomogeneity. The high carbon content makes probable that at least part of this extensive contamination resulted from the outgassing of the graphite heating element since the calorimeter had not been used for some time.

In contrast, the second run in the SETARAM calorimeter showed orderly behavior during the majority of the drops with the time dependence of the temperature difference between the bath and heat reservoir showing a monotonic change in pattern with each successive drop. A definite deviation from the monotonically changing pattern began with the fifth last sample and became worse with each additional sample. This resulted in the last five data points from concentrations of  $X_{Ti} > 0.5$  (where  $X_{Ti}$  is the mole fraction of Ti) being discarded. Whether or not additional points toward the end of the run should be discarded is considered in the discussion section. Post-run examination of the solidified metal showed a solid, homogeneous mass without pipes or voids. Chemical analyses again indicated increase in content of interstitial elements. The analyses from this second run are included in Table 1, and comparison with the analyses from the first run shows the contamination by oxygen, hydrogen, and nitrogen in the two runs to be roughly comparable but the carbon contamination during the second run to be markedly less.

It is believed that the excess carbon contamination during the first run occurred early in the run and was responsible for the pipes, voids, and

TABLE 2

Experimental values for the heats of mixing,  $\Delta_m H$ , of liquid Ni-Ti alloys, for the function  $\xi$  where  $\xi$  is  $\Delta_m H/X_{Ti}X_{Ni}$ , and for the function  $\xi_{mod}$  where  $\xi_{mod}$  is  $\xi[X_{Ti}(r_{Ti}/r_{Ni}) + X_{Ni}(r_{Ni}/r_{Ti})]^2$

$X_{Ti}$	$-\Delta_m H$ (kJ mol <sup>-1</sup> )	$-\xi$ (kJ mol <sup>-1</sup> )	$-\xi_{mod}$ (kJ mol <sup>-1</sup> )
<i>Data from the high vacuum calorimeter at 1838 K</i>			
0.0422	8 318	205.8	157.7
0.0786	14 795	204.3	161.1
0.1310	23 513	206.5	169.4
0.1782	29 230	199.6	169.5
0.2195	33 951	198.2	173.3
0.2562	37 800	198.3	177.8
0.3062	40 522	190.7	176.8
0.3419	40 761	181.2	172.0
<i>Data from the SETARAM calorimeter at 1741 K</i>			
0.0971	18.15	207.0	165.6
0.1783	28.97	197.8	168.0
0.2443	36.54	197.9	176.0
0.3008	40.43	192.3	177.7
0.3546	42.42	185.4	177.4
0.3914	42.49	178.4	174.6
0.4286	41.95	171.3	171.6
0.4619	41.13	165.5	169.2
0.4918	40.17	160.7	167.2

erratic behavior that was observed. On the other hand, it is probable that the contamination by oxygen and possibly nitrogen occurred later in both runs and was responsible for the need to discard the last five points of the second run. Support for this view comes from two sources. First, the interface appearing in the cross-section, after slicing vertically through the combined crucible and solidified melt of the second run, showed signs of reaction at the interface, and the interface is a logical place to generate oxygen contamination after the Ti activity has become sufficiently high. Second, comparison of the analytical data in Table 1 from the second SETARAM run with data from the run in the vacuum calorimeter shows that contamination in the vacuum calorimeter was much less, yet comparison of the calorimetric results from the two runs shows generally good agreement up to the maximum Ti concentration reached in the vacuum calorimeter. The level of agreement can be seen from the information in Table 2 and is even more obvious from the plot in Fig. 2. This agreement between the two runs at compositions in the Ni-rich portion of the system together with the difference in analytical data in Table 1 supports the view that oxygen and/or nitrogen contamination is responsible for any difference between the runs, specifically the aberrant nature of the last five points of the second

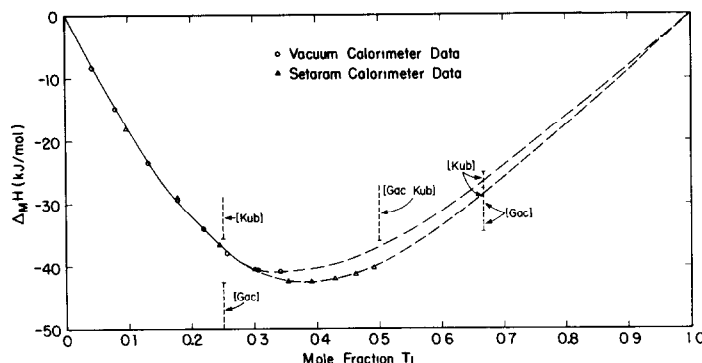


Fig 2 Experimental values from two sets of independent calorimetric measurements of the enthalpies of mixing of liquid Ni-Ti alloys as a function of the mole fraction of Ti Extrapolated values at the compositions of the three solid intermetallic phases from measurements on solid alloys from Kubaschewski [Kub] and from Gachon, Notin and Hertz [Gac] are included for comparison

**SETARAM run** Further, the excess contamination in the second SETARAM run most likely occurred late in the run

Only one run was made in the vacuum calorimeter Post-run examination of the solidified metal showed a massive, homogeneous piece of metal, and analytical data in Table 1 show a slight increase in O content when compared to the analyses of the uncombined elements but no significant increase in H, N, or C content The terminal Ti content, and thence the Ti activity reached during the measurements in the vacuum calorimeter were somewhat below those reached during the second run in the SETARAM calorimeter As noted above, this supports the view that contamination in the SETARAM calorimeter occurred predominately during the last five drops

## DISCUSSION

Figure 1 shows the most exothermic heat of mixing of the liquid alloys to be below  $X_{Ti} = 0.4$  In comparison, a regular solution would exhibit this extremum at  $X_{Ti} = 0.5$  Thus, Ni-Ti liquid solutions are not regular, and this is shown more definitively in Fig 3(a) where  $\xi = \Delta_m H / (X_{Ni} X_{Ti})$  is plotted against  $X_{Ti}$  This function should be a constant for a regular solution, and the plot would be a horizontal straight line The plot which the actual experimental data changes slope in the vicinity of  $X_{Ti} = 0.3$  and thus indicates possible short-range order or association in the region above the highly stable  $Ni_3Ti$  phase To determine whether the irregularity of the liquid solution is in fact caused by short-range order or if it is mainly due to the size difference between the atomic species and to atomic packing effects

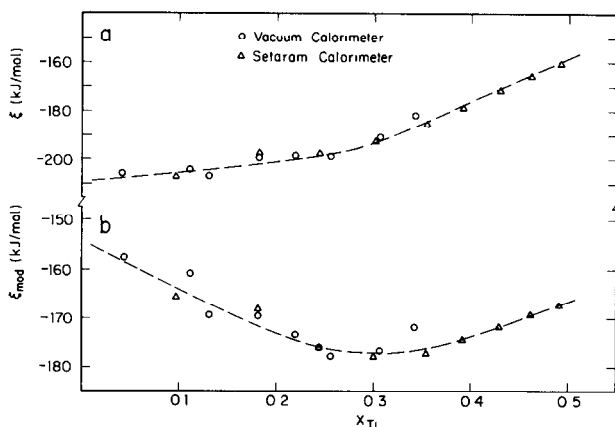


Fig 3 (a) Compositional dependence of the function  $\xi = \Delta_m H / X_{Ti} X_{Ni}$  and (b) compositional dependence of the function  $\xi_{mod} = \xi [X_{Ti}(r_{Ti}/r_{Ni}) + X_{Ni}(r_{Ni}/r_{Ti})]^2$

$\xi_{mod} = \xi [X_{Ti}(r_{Ti}/r_{Ni}) + X_{Ni}(r_{Ni}/r_{Ti})]^2$  is plotted against  $X_{Ti}$  in Fig 3(b). This equation has been derived assuming that the different mean coordination numbers can be approximated by the different surfaces of the atomic species. This simple approximation is achieved by replacing the atomic fractions by the fractions of the atomic surfaces; this approximation is sufficient if the ratio of the atomic radii is less than about 1.5 (i.e. the relation does not hold for interstitials). With this simple approximation, a regular solution of atoms with different radii requires a plot of  $\xi_{mod}$  vs  $X_{Ti}$  to be a straight horizontal line. A more sophisticated and fundamental derivation also results in a linear relationship for a regular solution but with slope a priori unknown.

In the present case, the values of  $r_{Ti}/r_{Ni}$  is 1.162 and represents the radius ratio [30] of the atomic species. This plot shows a minimum that, like the break in Fig. 3(a), is near  $X_{Ti} = 0.3$ . It is thus highly probable that effects of atomic packing efficiency are influencing the energetics of the system. Obviously, such effects from packing considerations would also result in some degree of short-range order.

Gachon and Hertz [22] reported the following values for the enthalpies of formation of the three solid intermediate phases:  $-49.2 \pm 1$  at 1513 K for  $Ni_3Ti$ ,  $-34.0 \pm 2$  at 1475 K for  $NiTi$ , and  $-29.3 \pm 0.5$  at 1202 K for  $NiTi_2$ , all in kJ (mol atoms) $^{-1}$ . In comparison, Kubaschewski [20] reported values of  $-34.7 \pm 2$  for  $Ni_3Ti$ ,  $-33.9 \pm 2$  for  $NiTi$ , and  $-26.8 \pm 2$  for  $NiTi_2$ , again in kJ (mol atoms) $^{-1}$  and all at 298 K. Because of the lack of heat capacity data and heats of fusion for all but the elemental components, comparison of these results for the solid alloys with the present results for the liquid alloys requires approximations that leave comparatively large uncertainties. First,  $\Delta C_p$  effects for both solids and liquids were neglected as also were any



contributions from the allotropic transition in Ti or from the solid state transition in NiTi. The enthalpies of formation of the solid alloys and the enthalpies of mixing of the liquid alloys were thus assumed to be temperature independent. Converting the enthalpies of formation of the solid alloys to enthalpies of mixing of the corresponding liquid alloys is then a matter of adding a correction for the difference between the heat of fusion of the alloy and the weighted heats of fusion of the elemental components.

Heats of fusion for the elements are available [27] but must be estimated for the alloys. This was done by estimating the entropies of fusion as being composed of two parts. One part was considered to arise from the change associated with vibrational randomness being converted to convectional randomness and was evaluated as the compositionally weighted average of the elemental values. The second part was the onset of additional configurational randomness and was bracketed as between zero and the ideal entropy of mixing at the stoichiometry in question. This bracketing allowed for some configurational randomness to pre-exist in the solid before melting or for the persistence of some order into the liquid. The entropies were converted to enthalpies by multiplication with the melting temperature. With this procedure and the Gachon-Hertz data, the brackets for the enthalpies of mixing are  $-42.5$  to  $-50.3$  for  $\text{Ni}_3\text{Ti}$ ,  $-26.9$  to  $-36.0$  for  $\text{NiTi}$ , and  $-27.6$  to  $-34.3$  for  $\text{NiTi}_2$ , again in  $\text{kJ (mol atoms)}^{-1}$ . Brackets for the Kubaschewski data are  $-28.0$  to  $-35.8$  for  $\text{Ni}_3\text{Ti}$ ,  $-26.8$  to  $-35.9$  for  $\text{NiTi}$ , and  $-25.1$  to  $-34.3$  for  $\text{NiTi}_2$ . These ranges are shown by the vertical bars at appropriate compositions in Fig. 2. The figure shows that the present experimental data near the composition  $\text{Ni}_3\text{Ti}$  pass between the ranges predicted from the Gachon-Hertz and Kubaschewski measurements.

Since the last five points in the second SETARAM run were discarded as aberrant with evidence favoring oxygen and/or nitrogen contamination as the cause, there is a question as to whether or not additional points should be dropped. Certainly reaction with oxygen or nitrogen would release extra heat, and there is a hint that the last five points may be slightly too negative since the last point from the vacuum calorimeter run deviates toward the high side of the last five SETARAM points. However, there is no guarantee that this high point is not the one that is aberrant. In Fig. 2 the two curves extrapolating the experimental points into the Ti-rich region are visual fits and were drawn with the constraint that there should be no inflection points. Visual fits were used because a number of two and three parameter least-squares analytical fits were tried both with the twelve points terminating at the last vacuum calorimeter point and with all seventeen data points, however, these analytical fits were not satisfactory.

Examination of the visually-extrapolated curves shows that they both pass reasonably close to or through the bracketed ranges predicted for  $\text{NiTi}$  and  $\text{NiTi}_2$  from the Gachon-Hertz and Kubaschewski measurements. On this basis there appears no solid basis for discarding the last five SETARAM

points, at the most they are too negative by about  $2 \text{ kJ (mol atoms)}^{-1}$  which is within experimental uncertainty

## ACKNOWLEDGMENTS

The authors are indebted to John Wheelock and Marvin Thompson of the Ames Laboratory for preparing the samples and to Herr W. Furmanski for his assistance during the SETARAM calorimetric measurements. The contribution of Herr H. Opielka and Frau B. Stark is also gratefully acknowledged. The calorimetric measurements were carried out at the MPI für Metallforschung, Stuttgart, F.R.G. One of us (J.F.S.) is indebted to Iowa State University for leave during this period and to the Max-Planck Society for financial support.

## REFERENCES

- 1 D.M. Poole and W. Hume-Rothery, *J. Inst. Metals*, 83 (1959) 473
- 2 A. Taylor and R.W. Floyd, *Acta Crystallogr.*, 3 (1950) 285
- 3 A. Taylor and R.W. Floyd, *J. Inst. Metals*, 80 (1951-2) 577
- 4 F. Laves and H.J. Wallbaum, *Naturwissenschaften*, 27 (1939) 674
- 5 F. Laves and H.J. Wallbaum, *Z. Kristallogr.*, 10 (1939) 78
- 6 H.J. Wallbaum, *Arch. Eisenhüttenwes.*, 12 (1938-9) 299
- 7 P. Duwez and J.L. Taylor, *Trans. Am. Inst. Min. Met. Eng.*, 188 (1950) 173
- 8 W. Rostoker, *Trans. Am. Inst. Min. Met. Eng.*, 191 (1951) 1203
- 9 R.J. Wasilewski, *Trans. Am. Inst. Min. Met. Eng.*, 233 (1965) 1691
- 10 N.G. Pace and G.A. Saunders, *Solid State Commun.*, 9 (1971) 331
- 11 F.E. Wang, W.J. Buehler, and S.J. Pickart, *J. Appl. Phys.*, 36 (1965) 3232
- 12 D.K. Rehbein, B.J. Skillings, J.F. Smith, and D.O. Thompson, *J. Nondestruct. Eval.*, 4 (1984) 3
- 13 D.E. Polk, A. Calk, and B.C. Giessen, *Acta Metall.*, 26 (1978) 1097
- 14 K.H.J. Buschow and N.M. Beckmans, *J. Appl. Phys.*, 50 (1979) 6348
- 15 K. Zoltzer and R. Bormann, *J. Less-Common Met.*, 140 (1988)
- 16 Z. Zhang, H.Q. Ye, and K.H. Kuo, *Phil. Mag. Part A*, 52 (1985) L49
- 17 D.P. Dautovich, Z. Melkvi, G.R. Purdy, and C.V. Stager, *J. Appl. Phys.*, 37 (1966) 2513
- 18 R.J. Wasilewski, S.R. Butler, and J.E. Hanlon, *Met. Sci.*, 1 (1967) 104
- 19 H.A. Berman, D. West, and A.G. Rozner, *J. Appl. Phys.* 38 (1967) 4473
- 20 O. Kubaschewski, *Trans. Faraday Soc.*, 54 (1958) 814
- 21 J.C. Gachon, M. Notin and J. Hertz, *Thermochim. Acta*, 48 (1981) 155
- 22 J.C. Gachon and J. Hertz, *Calphad*, 7 (1983) 1
- 23 O.J. Kleppa, in Y.A. Chang and J.F. Smith (Eds.), *Calculation of Phase Diagrams and Thermochemistry of Alloy Phases*, The Metallurgical Society-AIME, Warrendale, PA, 1979, 213
- 24 M.J. Pool, B. Predel, and E. Schultheiss, *Thermochim. Acta*, 28 (1979) 349
- 25 I. Arpshofen, B. Predel, E. Schultheiss and M. Hoch, *Thermochim. Acta*, 33 (1979) 197
- 26 R. Luck and B. Predel, *Z. Metallkd.*, 76 (1985) 684

- 27 R Hultgren, P D Desai, D T Hawkins, M Gleiser, K K Kelley and D D Wagman, Selected Values of the Thermodynamic Properties of the Elements, Am Soc Metals, Metals Park, Ohio 1973
- 28 C E Wicks and F E Block, U S Bur Mines Bull , 605 (1963), 11, 84, 121
- 29 O Kubaschewski and C B Alcock, Metallurgical Thermochemistry, 5th edn , Pergamon, New York, 1979
- 30 E Fluck and Th Heumann, Periodensystem der Elemente, VCH Verlagsgesellschaft, Weinheim, 1985